International Journal of Thermophysics, Vol. 7, No. 1, 1986

Simultaneous Measurement of Thermal Diffusivity and Specific Heat at High Temperatures by a Single Rectangular Pulse Heating Method[1]

K. Kobayasi[2]

A method for the simultaneous measurement of thermal diffusivity and specific heat by a single rectangular heating pulse on a finite cylindrical specimen is described. The method takes into account radiation losses from all the surfaces of the specimen. The theoretical principle of the technique was studied by solving the transient heat conduction equation for a finite disk heated on the front surface by a single rectangular radiant energy pulse. An apparatus was constructed to comply with the theoretical conditions and was connected to a personal computer. Thermal diffusivity and specific heat were determined from the data obtained on the temperature response of the back surface of the specimen and from the theoretical results. This method can be applied to materials having a wide range of thermal conductivity values and has a good accuracy at high temperatures. Examples of the measurements are presented.

KEY WORDS: high temperatures; pulse heating; specific heat; thermal conductivity; thermal diffusivity.

1. INTRODUCTION

There are no definite techniques to measure a wide range of thermal conductivity values and temperatures with only one apparatus. The conventional technique that utilizes steady-state heat flow takes too much time for measurements and is subject to difficulties which increase with increasing temperature. These difficulties are due to the problems associated with maintaining proper steady state conditions at high temperatures.

[1] Invited paper presented at the Ninth Symposium on Thermophysical Properties, June 24–27, 1985, Boulder, Colorado, U.S.A.

[2] Department of Mechanical System Engineering, Toyota Technological Institute, 2-12-1 Hisakata, Tempaku-ku, Nagoya 468, Japan.

0195-928X/86/0100-0181$05.00/0

Cowan [1] conducted theoretical studies on transient methods for an infinite slab by stepwise, pulsewise, and periodic heating for determining thermal diffusivity. His conclusion was that the stepwise heating method would probably yield poor results.

On the other hand, Parker et al. [2] reported a transient method which yielded thermal diffusivity from the measurements of the temperature response of the specimen after being irradiated with a light flash and demonstrated the possibility of short time measurements. This method has been modified and used by many researchers, e.g., Refs. 3 and 4; various pulse radiant energy sources, including lasers, have been and continue to be used. However, this technique is not suitable for measurements on materials with a low thermal conductivity, such as nonmetals and ceramics, due to the fact that in those cases the total absorbed energy resulting from the pulse radiation is small.

This author and other investigators developed a measuring technique by the stepwise heating method, taking into account radiation heat loss from the specimen [5–11].

In this paper, the theoretical principle is presented for the simultaneous measurement of thermal diffusivity and specific heat by a single rectangular heating pulse on a finite cylindrical specimen, taking into account radiation losses from all of its surfaces. The development of an apparatus that can be used for materials having a wide range of thermal conductivities and is accurate at high temperatures is also presented.

2. MEASUREMENT THEORY

2.1. Thermal Diffusivity

As shown in Fig. 1 we assume that the front surface ($x = l$) of a disk-shaped specimen, which is in vacuum and is in thermal equilibrium with the ambient temperature T_0, is heated by a single rectangular radiant heat pulse with intensity H_0/ε_l and time width δ, where ε_l denotes the emissivity of the front surface. Under these conditions, we investigated a method to find the thermal diffusivity and specific heat by the temperature rise of the rear surface ($x = 0$) of the specimen. Heat losses from the specimen by convection and conduction may be neglected when it is in vacuum.

The solution for finding the temperature rise, when the specimen is heated by a single rectangular pulse of width δ, is obtained by subtracting the solution resulting from stepwise heating at $t = \delta$ from the solution resulting from the same heating at $t = 0$.

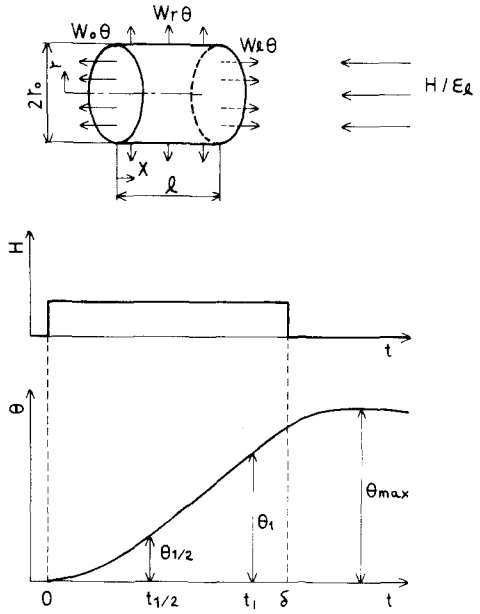

Fig. 1. Schematic diagram of the method of heating of a single rectangular pulse on a finite-cylindrical specimen.

The fundamental equation and initial and boundary conditions for the case of stepwise heating of the specimen at $t=0$ are expressed as follows:

$$\frac{\partial\theta}{\partial t}=a\left(\frac{\partial^2\theta}{\partial r^2}+\frac{1}{r}\frac{\partial\theta}{\partial r}+\frac{\partial^2\theta}{\partial x^2}\right) \qquad (0<x<l) \tag{1}$$

$$\lambda\frac{\partial\theta}{\partial x}=W_0\theta \qquad (x=0) \tag{2}$$

$$\lambda\frac{\partial\theta}{\partial x}=H_0-W_l\theta \qquad (x=l) \tag{3}$$

$$\lambda\frac{\partial\theta}{\partial r}=-W_r\theta \qquad (r=r_0) \tag{4}$$

$$\lambda\frac{\partial\theta}{\partial r}=0 \qquad (r=0) \tag{5}$$

$$\theta=0 \qquad (t\leqslant 0) \tag{6}$$

where θ, t, a, x, r, r_0, and λ express the temperature difference, time, thermal diffusivity, axial and radial coordinates, radius of the specimen, and thermal conductivity, respectively.

Heat absorbed at the front surface is denoted by H_0 and the radiation heat losses from the surfaces of the specimen are linearized as follows:

$$\varepsilon_x \sigma (T_0 + \theta)^4 - \varepsilon_x \sigma T_0^4 \simeq 4\varepsilon_x \sigma T_0^3 \theta = W_x \theta \tag{7}$$

because the temperature rise θ is small compared with T_0, i.e., $\theta \ll T_0$, where ε_x, σ, and W_x express the emissivity ($x = 0, l, r$), Stefan–Boltzmann constant, and $W_x = 4\varepsilon_x \sigma T_0^3$, respectively.

If we choose nondimensional quantities as follows,

$$\begin{aligned} &\Theta = \theta/(H_0 l/\lambda), \qquad R = r/r_0, \qquad X = x/l \\ &F_0 = at/l^2, \qquad B_0 = W_0 l/\lambda, \qquad B_l = W_l l/\lambda \\ &B_r = W_r r_0/\lambda, \qquad \gamma_0 = r_0/l \end{aligned} \tag{8}$$

where F_0 and B_x ($x = 0, l, r$) denote the Fourier and Biot numbers and γ_0 is the radius-to-thickness ratio of the specimen, Eqs. (1)–(6) are expressed as follows:

$$\frac{\partial \Theta}{\partial F_0} = \frac{1}{\gamma_0^2}\left(\frac{\partial^2 \Theta}{\partial R^2} + \frac{1}{R}\frac{\partial \Theta}{\partial R}\right) + \frac{\partial^2 \Theta}{\partial X^2} \qquad (0 < X < 1) \tag{9}$$

$$\frac{\partial \Theta}{\partial X} = B_0 \Theta \qquad (X = 0) \tag{10}$$

$$\frac{\partial \Theta}{\partial X} = 1 - B_l \Theta \qquad (X = 1) \tag{11}$$

$$\frac{\partial \Theta}{\partial R} = -B_r \Theta \qquad (R = 1) \tag{12}$$

$$\frac{\partial \Theta}{\partial R} = 0 \qquad (R = 0) \tag{13}$$

$$\Theta = 0 \qquad (F_0 \leqslant 0) \tag{14}$$

The solution of Eq. (9) for the conditions given by Eqs. (10)–(14) is obtained as follows [5]:

$$\Theta(R, X, F_0) = \sum_{n=1}^{\infty} \frac{2B_r J_0(w_n R)}{(w_n^2 + B_r^2) J_0(w_n)} \left\{ \frac{u_n \cosh(u_n X) + B_0 \sinh(u_n X)}{\alpha u_n \cosh u_n + (\beta + u_n^2) \sinh u_n} - 2 \sum_{m=1}^{\infty} \frac{v_m \cos(v_m X) + B_0 \sin(v_m X)}{(u_n^2 + v_m^2) D_m} \times \exp[-(u_n^2 + v_m^2) F_0] \right\} \tag{15}$$

where w_n is the nth root of

$$wJ_1(w) - B_r J_0(w) = 0 \tag{16}$$

and v_m is the mth root of

$$\alpha v \cos v + (\beta - v^2) \sin v = 0 \tag{17}$$

and the parameters are expressed as follows:

$$u_n = w_n / \gamma_0 \tag{18}$$

$$\alpha = B_0 + B_l \tag{19}$$

$$\beta = B_0 B_l \tag{20}$$

$$D_m = \sin v_m [1 + \alpha - (2\beta/\alpha) + (v_m^2/\alpha) + (\beta/v_m^2) + (\beta^2/\alpha v_m^2)] \tag{21}$$

Similarly, the solution resulting from stepwise heating at $t = \delta$ is obtained by substitution of $(t - \delta)$ for t in Eq. (15) as follows:

$$\Theta(R, X, F_0 - F_\delta) = \sum_{n=1}^{\infty} \frac{2B_r J_0(w_n R)}{(w_n^2 + B_r^2) J_0(w_n)} \left\{ \frac{u_n \cosh(u_n X) + B_0 \sinh(u_n X)}{\alpha u_n \cosh u_n + (\beta + u_n^2) \sinh u_n} - 2 \sum_{m=1}^{\infty} \frac{v_m \cos(v_m X) + B_0 \sin(v_m X)}{(u_n^2 + v_m^2) D_m} \times \exp[-(u_n^2 + v_m^2)(F_0 - F_\delta)] \right\} \tag{22}$$

where $F_\delta = a\delta / l^2$ is the Fourier number based on time width δ.

Therefore, the solution for the heating of a rectangular pulse is obtained by subtracting Eq. (22) from Eq. (15) as follows:

$$\Theta(R, X, F_0) - \Theta(R, X, F_0 - F_\delta) = 4 \sum_{n=1}^{\infty} \sum_{m=1}^{\infty} \frac{B_r J_0(w_n R)}{(w_n^2 + B_r^2) J_0(w_n)} \cdot \frac{v_m \cos(v_m X) + B_0 \sin(v_m X)}{(u_n^2 + v_m^2) D_m} \times \exp[-(u_n^2 + v_m^2) F_0] \{ \exp[(u_n^2 + v_m^2) F_\delta] - 1 \} \tag{23}$$

while Eq. (15) is still applicable for $0 \leqslant t \leqslant \delta$. Then the temperature rise at the center of the rear surface of the specimen is obtained as follows:

$$\Theta(0, 0, F_0) = \sum_{n=1}^{\infty} \frac{2B_r}{(w_n^2 + B_r^2) J_0(w_n)} \left\{ \frac{u_n}{\alpha u_n \cosh u_n + (\beta + u_n^2) \sinh u_n} - 2 \sum_{m=1}^{\infty} \frac{v_m}{(u_n^2 + v_m^2) D_m} \exp[-(u_n^2 + v_m^2) F_0] \right\}, \quad 0 \leqslant t \leqslant \delta \tag{24}$$

$$\Theta(0, 0, F_0) = 4 \sum_{n=1}^{\infty} \sum_{m=1}^{\infty} \frac{B_r}{(u_n^2 + v_m^2) J_0(w_n)} \cdot \frac{v_m}{(u_n^2 + v_m^2) D_m} \times \exp[-(u_n^2 + v_m^2) F_0] \{\exp[(u_n^2 + v_m^2) F_\delta] - 1\}, \quad t > \delta \tag{25}$$

If the emissivities are the same on all the surfaces of the specimen, $\varepsilon_0 = \varepsilon_l = \varepsilon_r$, we obtain

$$B_0 = B_l = \alpha/2 \tag{26}$$

$$B_r = B_0 \gamma_0 = \alpha \gamma_0 / 2 \tag{27}$$

$$\beta = \alpha^2/4 \tag{28}$$

Therefore, Eq. (24) becomes a function of F_0, with a parameter α, and

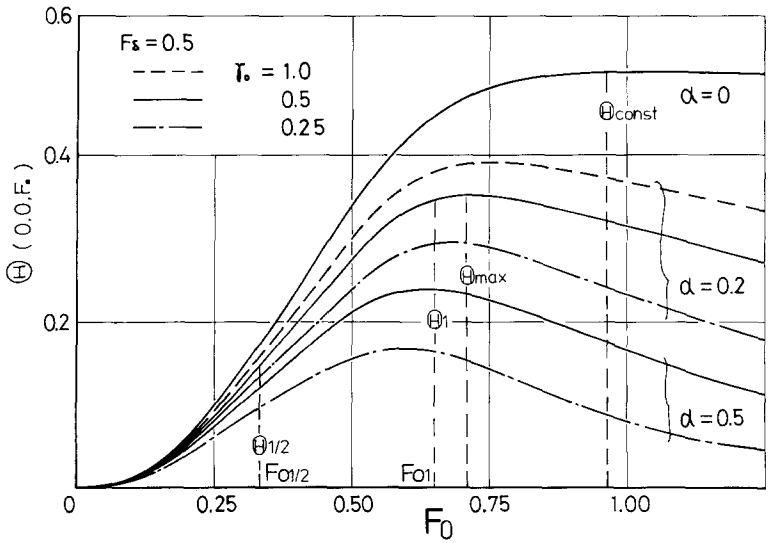

Fig. 2. Dimensionless temperature rise at the rear center of the specimen.

Eq. (25), with parameters α and F_δ, when the ratio γ_0 of the radius to the thickness of the specimen is given. Figure 2 shows an example of the theoretical temperature rise in this case, i.e., the curves in Fig. 2 show the calculation of the temperature rise at the center of the rear surface of the specimen versus dimensionless time F_0 in the case of $F_\delta = 0.5$ for three kinds of specimen shapes, $\gamma_0 = r_0/l = 1.0$, 0.5, and 0.25. The curve $\alpha = 0$ means the case without radiation loss from the specimen, and the loss increases according to $\alpha = 0.2$, 0.5. These curves are similar to those obtained in actual measurements. However, they are dimensionless temperature rises and include the heat flux H_0, which is unknown. So we selected two arbitrary times, t_1 and $t_{\frac{1}{2}}$, which corresponded to F_{01} and $F_{0\frac{1}{2}}$ on a curve, to eliminate H_0 so as to be

$$F_{01} = 2F_{0\frac{1}{2}} \tag{29}$$

and made a ratio of the temperature rise at the two Fourier numbers. Then, we obtained curves of the ratios of the temperature rise versus $F_{01}(\rightarrow F_0)$ as shown in Fig. 3. For any actual measurement, $F_0(=at_1/l^2)$ is determined from curves as in Fig. 3 after finding a ratio of $\theta_1/\theta_{\frac{1}{2}}$ by two

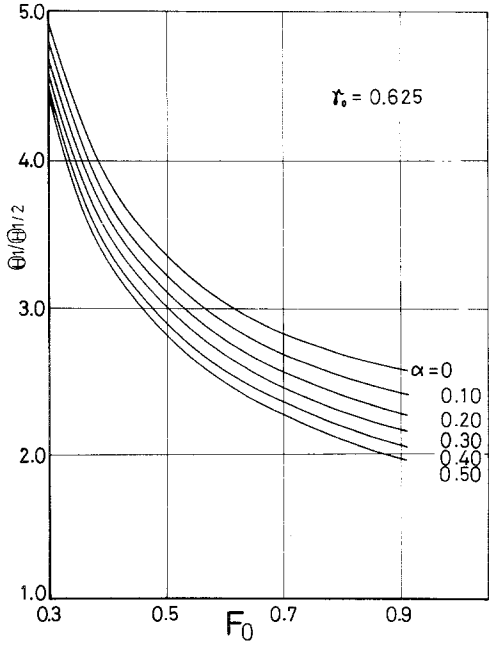

Fig. 3. Ratios of the temperature rise versus the Fourier number.

temperature rises, θ_1 and $\theta_{\frac{1}{2}}$, at arbitrary times t_1 and $t_{\frac{1}{2}}$ on a curve of temperature rise and a parameter α. Then, the thermal diffusivity a is obtained from F_0, as the specimen thickness l and time t_1 are known.

The radiation heat loss parameter α is expressed as follows:

$$\alpha = B_0 + B_l = 8\varepsilon_0 \sigma T_0^3 l/ac\rho \tag{30}$$

and this α includes a and c, which are also going to be measured. The way to find the value of α in such cases has already been published [5, 12]; i.e., we calculate α by using assumed values of a and c which are supposed to be the nearest values at first, find a from curves as in Fig. 3 by using this α next, and calculate α again by substituting the values of the second a and c into Eq. (30). The second c is found in another way described in the next section. We can obtain converged values of a, c, and α by making such iterations several times.

2.2. Specific Heat

Specific heat is determined from the known heat flux during the irradiation and the observed maximum temperature rise.

When the front surface of the specimen is heated by irradiation of a single rectangular pulse of width δ, the dimensionless temperature rise at the center of the rear surface of the specimen is given by Eq. (25). If we can neglect the radiation loss from the specimen, the temperature rise takes the value on the curve for $\alpha = 0$ and reaches a constant value $\Theta_{\text{const}}(\theta_{\text{const}})$ at $F_0 \to \infty (t \to \infty)$ as shown in Fig. 2. Therefore, the following equation is obtained in this case.

$$c = \frac{H_0 \delta}{\rho l \theta_{\text{const}}} \tag{31}$$

The heating flux H_0 is found beforehand by a similar operation using a reference specimen whose specific heat is well known [12].

If we cannot neglect the radiation heat loss from the specimen at high temperatures, the temperature rise takes curves with maximum value $\Theta_{\max}(\theta_{\max})$ as shown in Fig. 2. Then, specific heat c is expressed by the following equation, which includes a correction factor M

$$c = \frac{H_0 \delta}{\rho l \theta_{\max} M} \tag{32}$$

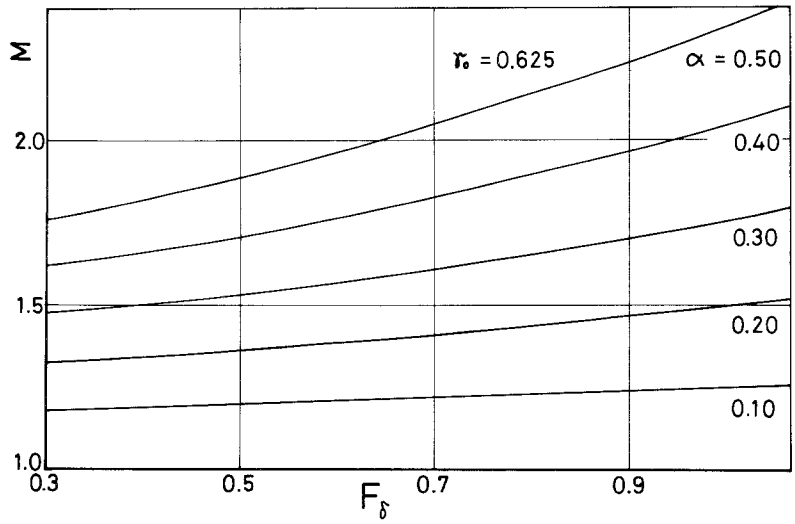

Fig. 4. Correction factor M versus Fourier number F_δ.

where

$$M = \frac{\theta_{\text{const}}}{\theta_{\max}} = \frac{\Theta_{\text{const}}}{\Theta_{\max}} \tag{33}$$

and $\Theta_{\max}$ and Θ_{const} express the dimensionless maximum temperature rise with and without the radiation heat loss from the specimen. Therefore, in theory, the factor M is given as a function of the variable F_δ with the parameter α for a definite γ_0. Figure 4 shows an example of the calculation of M. Then, specific heat c is determined from Eq. (32) by using $\theta_{\max}$, which is obtained from the measured temperature rise at the rear center of the specimen, and a correction factor M, which is determined from a curve theoretically similar to the one shown in Fig. 4, for F_δ, which is calculated with a value of thermal diffusivity a found in the way described in Section 2.1.

3. CONSIDERATION OF ACCURACY BASED ON THE SPECIMEN GEOMETRY FOR THE TWO THEORETICAL MODELS

Differences between the results of the two theoretical models for infinite-slab [12] and finite-cylinder specimens depend upon the radius-to-thickness ratio γ_0 of the specimen, the radiation heat loss parameter α, and

the Fourier number. The differences increase when the radiation heat loss and Fourier number increase and the radius-to-thickness ratio decreases.

Figure 5 shows an example of the temperature distribution progress in the specimen of $2\gamma_0 = 1.00$. It is clear that the effect of radiation heat loss from the side of the specimen increases with Fourier number increases. The heat loss affects the outer part larger than the center, but the differences between the two theoretical models increase even at the center of the specimen when the Fourier number increases. Therefore, large errors would be expected when the measured temperature rise is applied to the method based on an infinite-slab theory, in cases of small values of γ_0.

Further, it is recognized that the discrepancies between the real position of the temperature sensor and the center of the specimen do not severely affect the accuracy of the temperature response measurements when they are actually small.

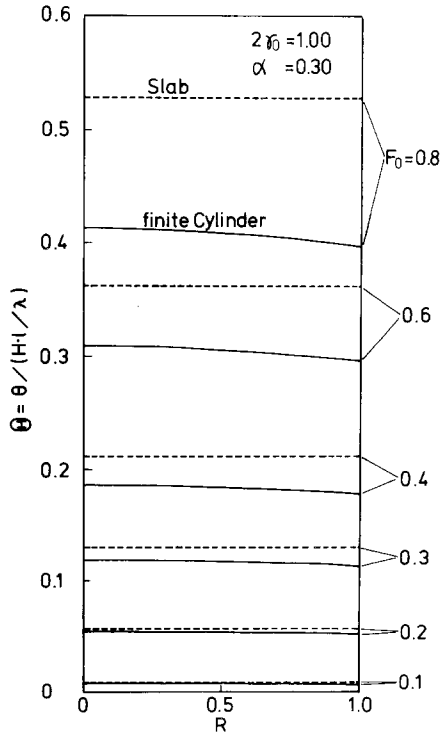

Fig. 5. Temperature distribution progress in the specimen.

In general, the effect of the radiation loss from the side of the specimen becomes so large for the cases $2\gamma_0 \leqslant 2.0$ that measurements based on the theory of an infinite slab will have large errors when the value of α is not small ($\alpha > 0.4$).

Although relative errors in the theoretical considerations of infinite-slab specimens compared to those of finite-cylinder specimens are about 9% for $2\gamma_0 = 2$ and $\alpha = 0.4$, for instance, the errors are decreased by the present consideration of finite-cylinder specimens.

4. APPARATUS

Figure 6 shows a schematic diagram of the apparatus of the measurement. A specimen, indicated by oblique lines, was located at the approximate center of a high-temperature electric furnace, which was evacuated to a pressure of 10^{-3} to 10^{-4} mm Hg by rotary and diffusion

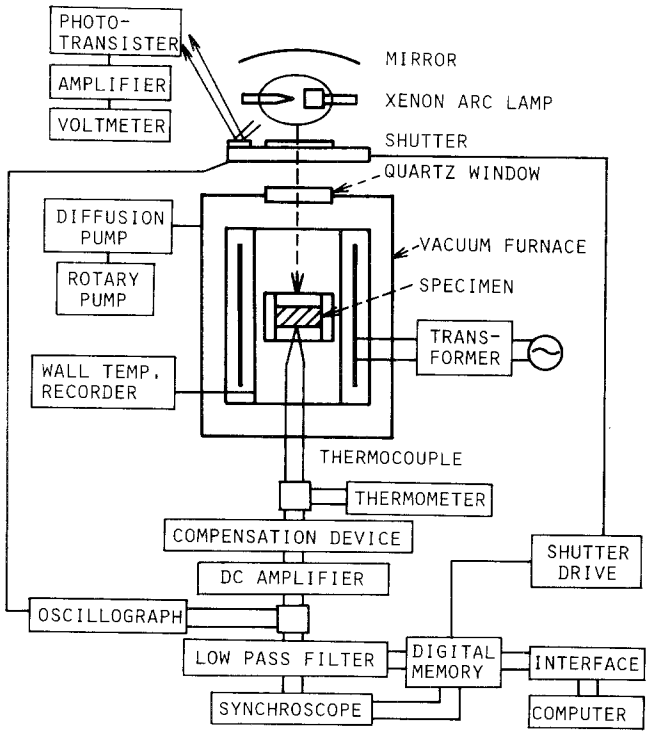

Fig. 6. Block diagram of the apparatus of the measurement by heating of a single rectangular pulse.

pumps. This effectively eliminates heat conduction and convection around the specimen, and its oxidation. After the specimen reached a thermal equilibrium state, the front surface was irradiated with a single rectangular pulse with time period δ obtained from a xenon arc lamp through a window and a shutter which had a timer. The time width of irradiation was usually 1 to 5 s and a run was completed within several seconds. The radiation pulse was focused on the specimen by a parabolic mirror to have a uniform intensity distribution in the beam cross section. All the surfaces of the specimen were coated with thin carbon black to make the emissivities equal.

The temperature rise at the center of the rear surface of the specimen was detected with a thin thermocouple and the signal was fed to the transient digital memory through a compensation device, a DC amplifier, and a low-pass filter. The purpose of the compensation device was to cancel out the thermoelectromotive force of the initial temperature so that only temperature rise was fed to the amplifier. The total temperature rise of the specimen after an irradiation was several degrees kelvin. The synchroscope, located in the parallel circuit, was used to confirm the curve of the temperature rise in the memory as occasion demanded. The curve was also recorded on an oscilloscope. The output from the digital memory was then fed to a computer through an interface. The thermal diffusivity a and the specific heat c were then simultaneously calculated by the process described before.

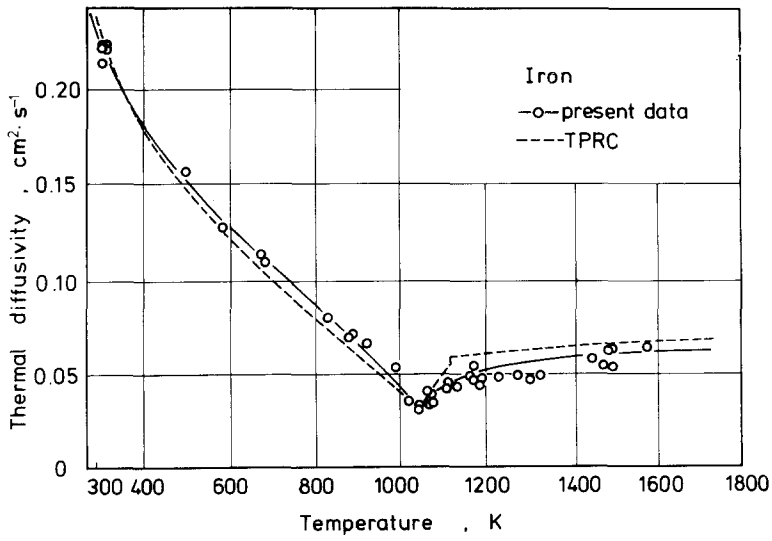

Fig. 7. Thermal diffusivity of electrolytic iron.

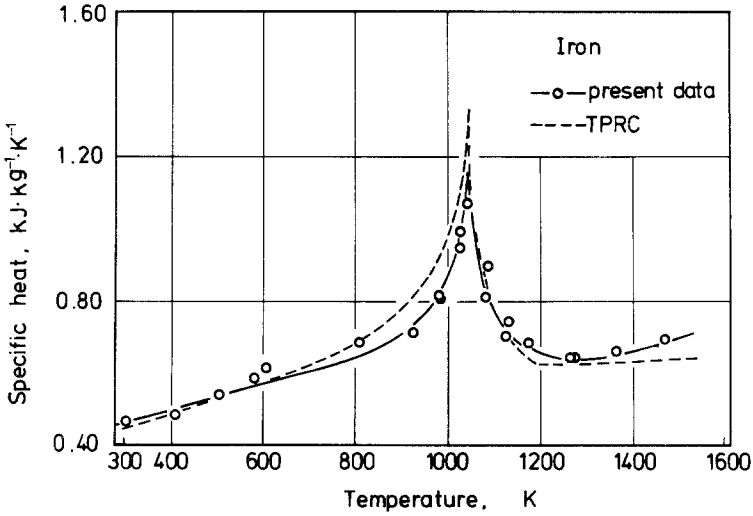

Fig. 8. Specific heat of electrolytic iron.

The combination of a phototransistor, an amplifier, and a voltmeter in Fig. 6 comprised a photometer which changed the reflected light into an electric signal to indicate the intensity of the radiant energy.

5. EXPERIMENTAL RESULTS

Figures 7 and 8 show the measurements of thermal diffusivity and specific heat of a high-purity electrolytic iron to check the performance of

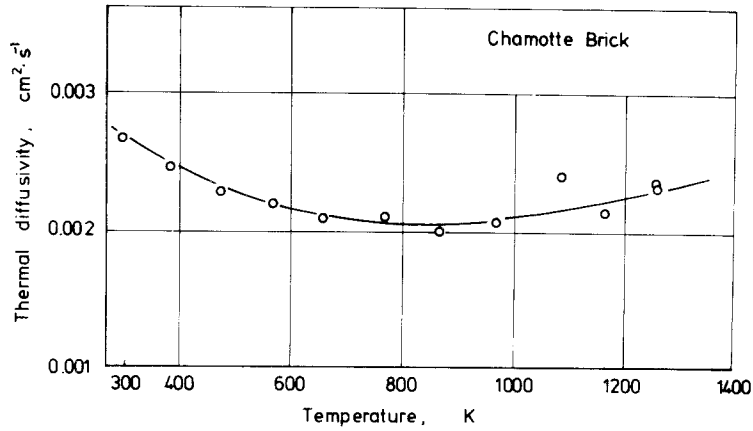

Fig. 9. Thermal diffusivity of a chamotte brick.

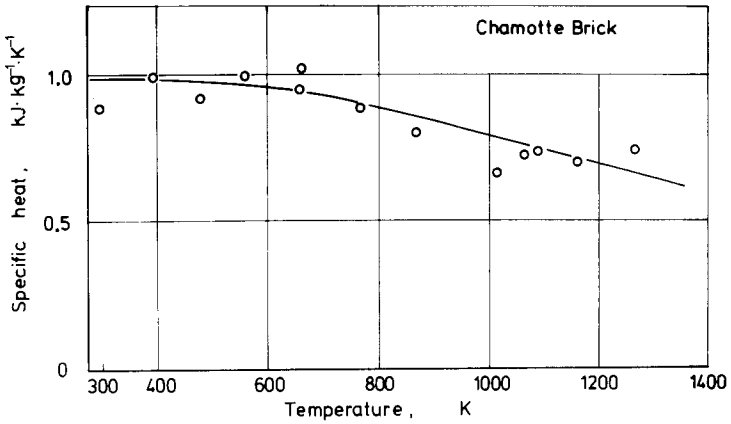

Fig. 10. Specific heat of a chamotte brick.

the apparatus and the method. The dashed line in Fig. 7 shows the recommended values by TPRC [14], which agree well with the present data in the range below the Curie point but are a little different above that point. The dashed line in Fig. 8 also shows the TPRC data [15], which agree with the present data fairly well.

Figures 9, 10, and 11 show the thermal diffusivity, the specific heat, and the thermal conductivity of a chamotte brick, as examples of the measurements. The apparent density of the sample was 1816 $kg \cdot m^{-3}$, and the thermal conductivity was calculated by the equation $\lambda = ac\rho$.

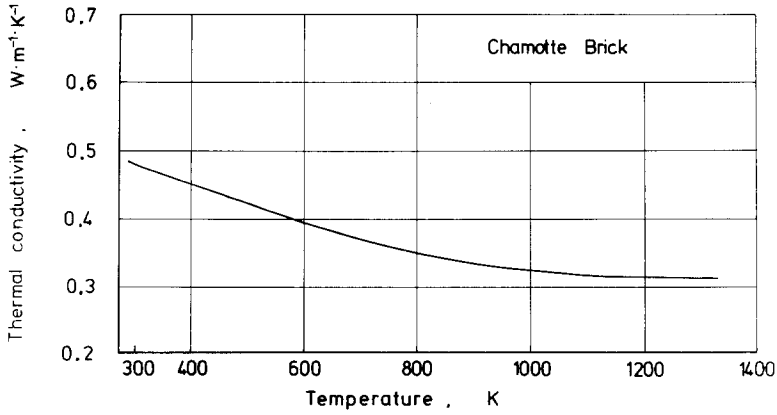

Fig. 11. Thermal conductivity of a chamotte brick.

6. CONCLUSION

A simultaneous measuring method of thermal diffusivity and specific heat by a single rectangular heating pulse on a finite-cylindrical specimen was theoretically studied with consideration of radiation heat losses from all the surfaces of the specimen.

Relative errors in the theoretical considerations between an infinite-slab specimen and a finite-cylindrical one depend upon the radius-to-thickness ratio γ_0 of the specimen, radiation heat loss parameter α, and Fourier number F_0. The errors are significant when γ_0 is small and α and F_0 are large, but they are lowered by the present method.

An apparatus complying with these theoretical results and connected to a personal computer was developed and some examples of the measurements are presented. The method and the apparatus made the measurements of thermal diffusivity and specific heat easy even for materials with a low thermal conductivity such as nonmetals and ceramics.

ACKNOWLEDGMENTS

The author wishes to extend his appreciation to Mr. T. Kobayashi and Mr. T. Takano for their assistance in the experiments and to the Ministry of Education of Japan for financial aid.

REFERENCES

1. R. D. Cowan, *J. Appl. Phys.* **32**:1363 (1961).
2. W. J. Parker et al., *J. Appl. Phys.* **32**:1679 (1961).
3. R. Taylor, *Br. J. Appl. Phys.* **16**:509 (1965).
4. J. B. Moser and O. L. Kruger, *J. Nucl. Mat.* **17**:153 (1965).
5. K. Kobayasi and T. Kumada, *J. Atom. Energy Soc. Jpn.* **9**:58 (1967).
6. T. Kumada and K. Kobayasi, *J. Atom. Energy Soc. Jpn.* **11**:462 (1969).
7. T. Kumada and K. Kobayasi, *J. Atom. Energy Soc. Jpn.* **11**:664 (1969).
8. T. Kumada and K. Kobayasi, *J. Nucl. Sci. Technol.* **9**:192 (1972).
9. K. Kobayasi and N. Araki, *Proc. 5th Int. Heat Transfer Conf., MAI* **3**(5):247 (1974).
10. Y. Kato, K. Kobayasi, N. Araki, and K. Furukawa, *J. Phys. Sci. Inst. E* **8**:461 (1975).
11. Y. Kato, K. Kobayasi, N. Araki, and K. Furukawa, *J. Phys. Sci. Inst. E* **10**:921 (1977).
12. K. Kobayasi and T. Kobayashi, *Trans. Jpn. Soc. Mech. Eng. B* **46**:1318 (1980).
13. K. Kobayasi, *J. Jpn. Soc. Mech. Eng.* **77**:754 (1974).
14. Y. S. Touloukian, R. W. Powell, C. Y. Ho, and M. C. Nicolaou, *Thermophysical Properties of Matter, Vol. 10. Thermal Diffusivity* (IFI/Plenum, New York, 1973), p. 82.
15. Y. S. Touloukian and E. H. Buyco, *Thermophysical Properties of Matter, Vol. 4. Specific Heat* (IFI/Plenum, New York, 1970), p. 102.